

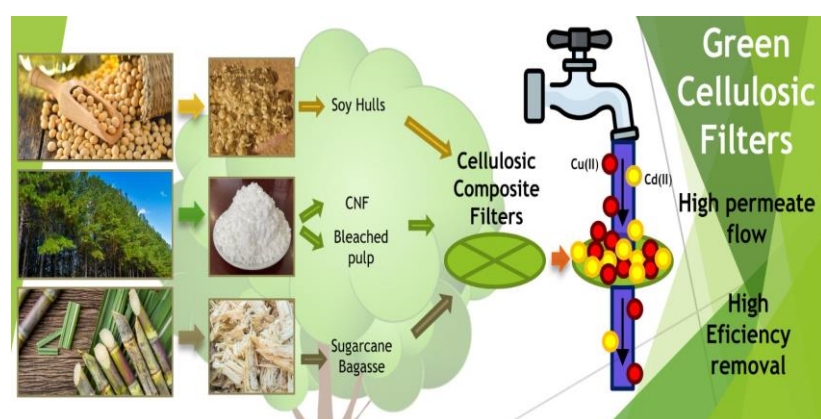
Full Paper | <http://dx.doi.org/10.17807/orbital.v16i2.19863>

Development of Agrowaste and Cellulose-based Composite Filters and Their Application in Fast Removal of Metallic Cations from Water

Pedro Eduardo Costa ^a, Altamiro Xavier de Souza ^b, Gabriel Badagnani de Carvalho ^a, Daniel Pasquini ^c, Marcelo Firmino de Oliveira ^d, Anizio Marcio de Faria ^e, Cláudio Roberto Neri ^d, and Luís Carlos de Morais* ^a

Low-cost lignocellulosic filters were made from soybean hulls (SH), sugarcane bagasse fibers (SBF), cellulose nanofibers (CNF), and Kraft-bleached pulp (BP) as renewable feedstocks and applied in Cu (II) and Cd (II) removal from aqueous medium. Filtration was performed with a vacuum pump; filtration times ranged from 3 to 1200 seconds. For the same filter, the best permeate flow was 13,333 L.h.m⁻² for both cations. The best Cd (II) removal (77.2 %) was achieved within 7 seconds at a permeate flow of 5,714 L.h.m⁻². The same filter was also the best at removing Cu (II) (46.5 %), which was achieved within 7 seconds at a permeate flow of 5,714 L.h.m⁻², as well. This short time evidenced that a long contact time is not needed to achieve higher removal. The best filter was made of BP, CNF, and SH. The presence of SBF and SH increased the contact angle and decreased the solid free energy surface. By FTIR-ATR it was possible to verify with which groups present in the chemical structures of the filter components the Cd (II) and Cu (II) cations interacted best. These results demonstrate the potential use of lignocellulosic biomass for producing composites aimed at water decontamination.

Graphical abstract



Keywords

Agrowaste
Cellulose Nanofibrils
Cellulosic-Composite Filters
Filtration
Metallic Cations
Water Purification

Article history

Received 12 Dec 2023
Revised 03 May 2024
Accepted 28 May 2024
Available online 29 June 2024

Handling Editor: Adilson Beatriz

^a Institute of Exact, Natural Sciences and Education (ICENE), Federal University of Triângulo Mineiro – UFTM, Uberaba, MG, Brazil. ^b Federal Institute of Education, Science, and Technology of São Paulo (IFSP), Sertãozinho Campus. 269 Américo Ambrósio Street, Jd Canaã, Zip Code: 14169-263, Sertãozinho-SP, Brazil. 1400 Randolpho Borges Júnior Avenue, Univerdecidade, Zip Code: 38064-200, Uberaba-MG. ^c Institute of Chemistry, Federal University of Uberlândia (UFU). 2121 João Naves de Ávila Avenue, Santa Mônica, Zip Code: 38400-902, Uberlândia-MG, Brazil. ^d Department of Chemistry, Faculty of Philosophy, Sciences, and Letters of Ribeirão Preto, University of São Paulo (FFCLRP/USP). Bandeirantes Av. 3900, USP Campus - Bairro Monte Alegre, Zip Code: 14040-900, Ribeirão Preto-SP, Brazil. ^e Institute of Exact and Natural Sciences of Pontal – ICENP – Federal University of Uberlândia (UFU). 1600 Rua Vinte – Bairro Tupã, Zip Code: 38304-402, Ituiutaba-MG, Brazil. *Corresponding author. E-mail: luis.morais@uftm.edu.br

1. Introduction

Millions of people do not have access to water with proper quality. This scenario has worsened as human activities grow without proper supervision. Although efforts have been made to alleviate this problem, they have not been enough. Indeed, the number and quantity of pollutants in lakes, rivers, and seas have risen. Unfortunately, once water is contaminated, obtaining good quality water becomes costly and takes a long time.

In this scenario, the major concern is the presence of pollutants in drinking water, including water contamination with small amounts of copper and cadmium. These metallic species have been associated with kidney and liver damage, human carcinogenesis, Wilson's disease, and insomnia [1]. The World Health Organization (WHO) recommends that cadmium and copper concentrations in drinking water be below 0.003 and 2 mg.L⁻¹, respectively [2].

Given that water is vital for human life, several methods have been employed to overcome aqueous contamination. In this sense, membranes are excellent materials for use in water purification. Cellulosic membranes have been applied to remove various contaminants, such as metallic ions and dyes [1,3-6] from water; good flow and removal efficiency have been reported.

Cellulose has been combined with other components to produce stable, low-cost cellulose-based composites that can remove metallic cations from water efficiently [7-9].

Agro-industrial residues are great sources of raw materials that can be explored to develop new composite materials for water purification, which can be applied in industrial wastewater treatment [10]. These so-called residues can form complexes with dyes [11], metallic ions [12,13], pesticides [14], and other aqueous contaminants. Moreover, they are inexpensive, and their annual production is high.

The materials produced from the agro-industrial residues have great potential for industrial activities.

This research did not aim to understand commonly used isotherm adsorption models such as Langmuir, Freundlich, and Sips, among many others. In these models, the conditions studied are not usually in flow, as occurs during the filtration process. The focus of this research was to study the removal of Cu (II) and Cd (II) contaminants during the continuous flow that occurs during the filtration process as dependence on the nature of the components present in each filter and the intrinsic aspects related to filtration and removal of these contaminants. Therefore, to better understand how metal cations interact with filter components, infrared spectroscopy was used. Thus, it was possible to evaluate which chemical groups interact with Cd (II) and Cu (II) based on the changes that occurred in the vibration modes of the chemical groups, either by noticeable signal displacement through the maximum region or by signal broadening, as discussed by other authors [15-18].

In this study, we aimed to produce cellulosic and lignocellulosic-based composite filters by employing cellulose nanofibers obtained from eucalyptus bleached Kraft pulp, bleached Kraft pulp fibers, sugarcane bagasse fibers, and soy hulls for application in Cu (II) and Cd (II) removal from water by a simple vacuum filtration process.

2. Results and Discussion

2.1 Bagasse and soy hull composition

The SBF and SH raw materials were of the same origin as those characterized by Silva *et al.* [19] and Neto *et al.* [20], respectively. Silva *et al.* described the total lignin (24.2 ± 0.360 %), hemicellulose (27.6 ± 0.070 %), and cellulose (42.8 ± 0.290 %) contents in SBF, and Neto *et al.* described the total lignin (5.78 ± 1.06 %), hemicellulose (24.0 ± 3.00 %), and cellulose (48.2 ± 2.10 %) contents in SH. For SH, the other components were protein, extractives, and ashes; for SBF, the other components were extractives and ashes.

2.2 SEM

Figure 1 shows the SEM surface and transversal view images of the composite filters. The SEM side view images of the filters allowed the thickness of the filters to be measured and their morphologies to be evaluated. The thickness values ranged from 80 to 120 μm ; the thinnest filter had the highest CNF content.

Images a, c, e, g, i, k, and m in Figure 1 showed that the top view of the filters with a larger amount of CNF exhibited fewer pores as compared to the filters containing a phase enriched with BP. The filters that contained more CNF tended to form layers deposited like lamellar structures (images b and l).

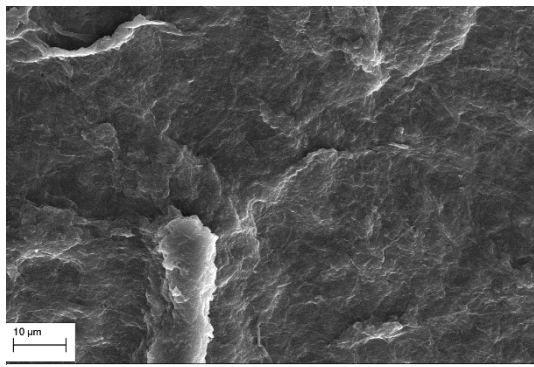
As reported by Putz *et al.* [21], when the vacuum is used as a deposition technique, the components tend to deposit in the same way as in the case of the self-assembly method, which supports the step depositions as layer-by-layer.

2.3 FTIR-ATR

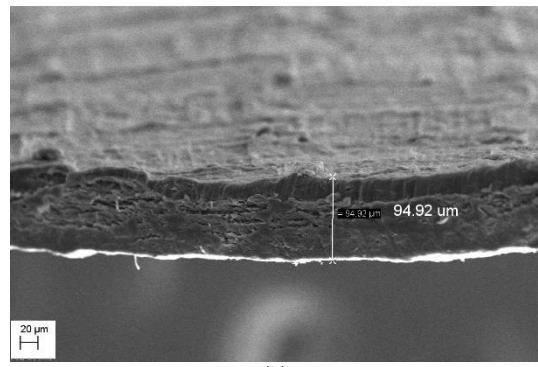
In Figure 2a-c, the ATR mode allowed us to identify the components in the filter as being of lignocellulosic origin.

The peaks that appeared in the range of 3200 to 3500 cm^{-1} corresponded to O-H bond stretching in cellulose, lignin, and hemicelluloses. The band near 2900 cm^{-1} was attributed to C-H bond stretching. The peak at 1316 cm^{-1} referred to $-\text{CH}_2$ stretching in cellulose, lignin, and hemicelluloses. The strong peak that emerged from 1140 to 900 cm^{-1} with a maximum near 1028 cm^{-1} was ascribed to C-O stretching in cellulose, lignin, and hemicelluloses. Finally, the peaks at 1158 and 900 cm^{-1} were assigned to C-O-C stretching of β (1-4) glycosidic bonds [22].

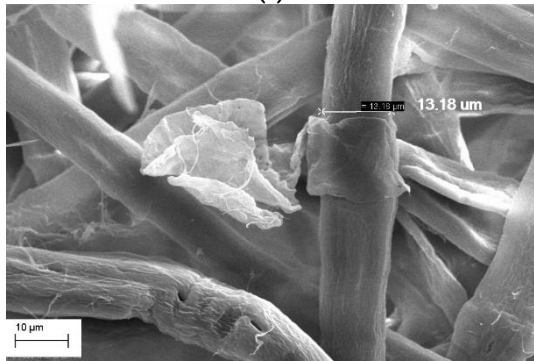
The peaks that arose from 1800 to 800 cm^{-1} showed the presence of lignin [23]. However, strong peaks referring to carbohydrates also appear in this region. The peak near 1310 cm^{-1} was due to syringyl and CH_2 stretching and bending, and the peak at 1640 cm^{-1} resulted from conjugated stretching of C=O in aromatic rings [24]. Generally, isolated lignin displays peaks at 1600, 1510, and 1440 cm^{-1} , associated with the vibration modes of the lignin aromatic ring. Nevertheless, these peaks were not visible because they are present in a wide band. The peak at 1640 cm^{-1} evidenced the presence of water, a very common component in polysaccharides [25, 26].



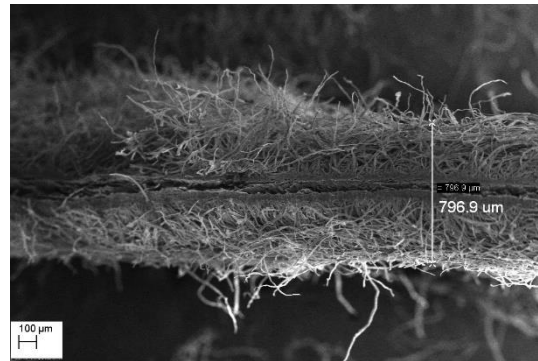
(a)



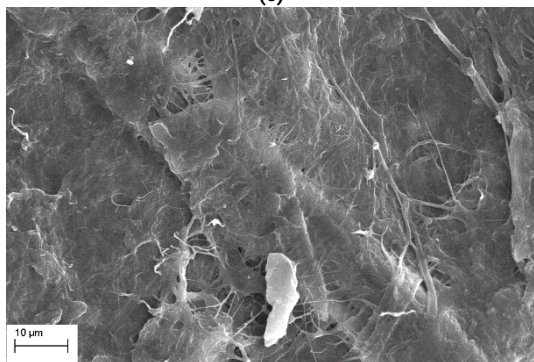
(b)



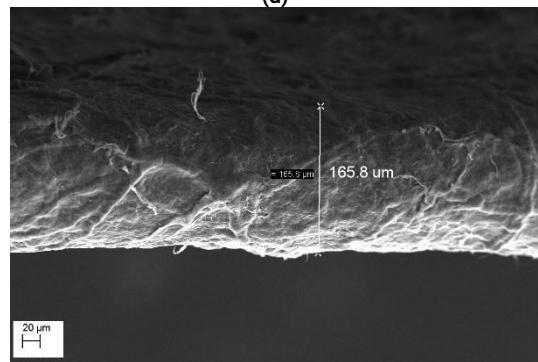
(c)



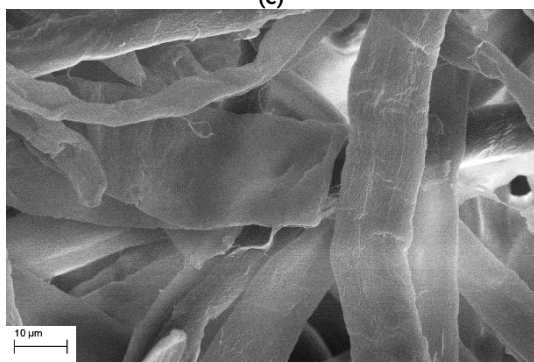
(d)



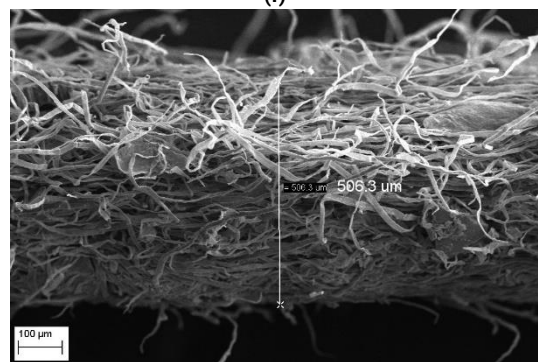
(e)



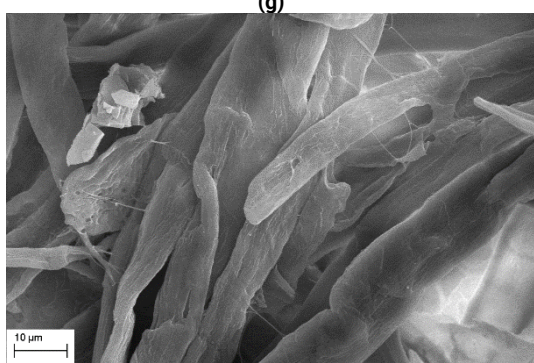
(f)



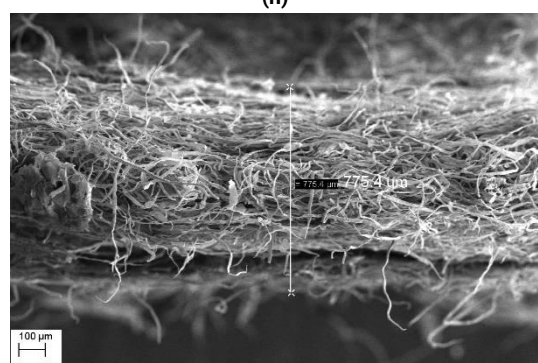
(g)



(h)



(i)



(j)

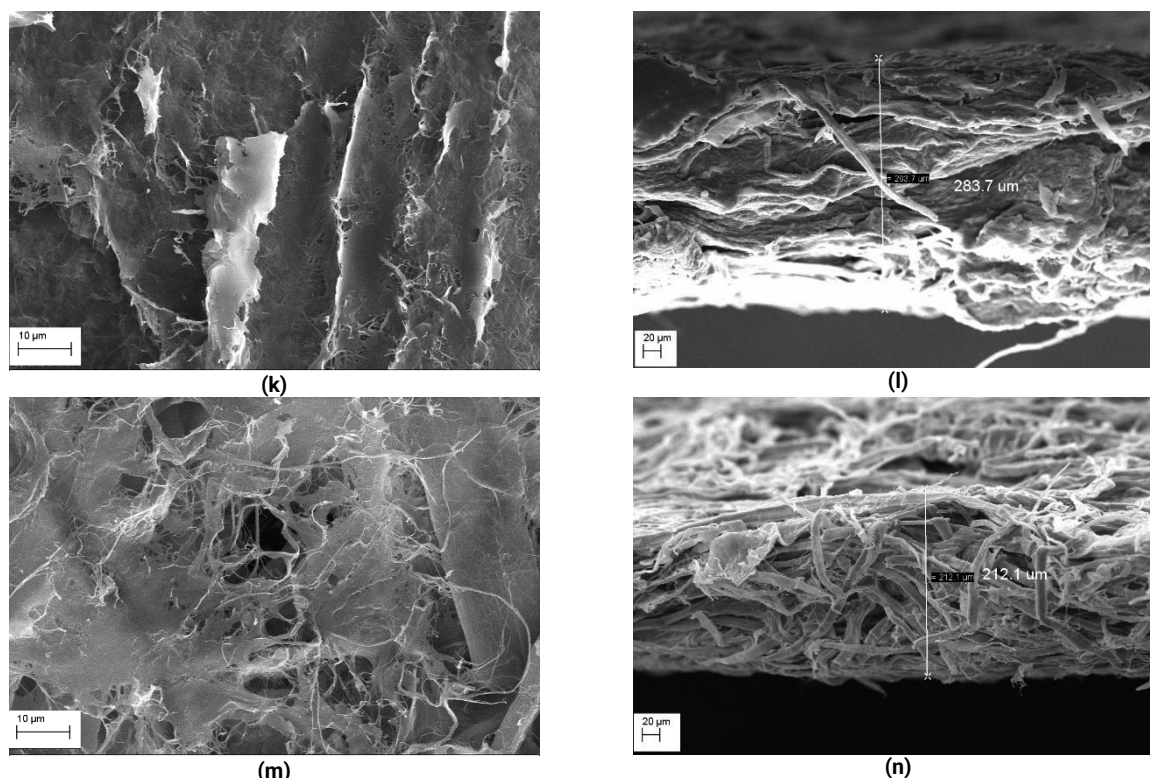


Fig. 1. SEM top (left) and transversal (right) view images of the filters. (a, b) CNF, (c,d) BP, (e,f) BP-CNF15, (g, h) BP-SH30, (i, j) BP-SBF30, (k, l), CNF-BP-SH30, and (m, n) BP-CNF-SH30. Magnifications of 500X (right) and 3 KX (left).

2.4 Contact angle

Several factors affect the contact angle measurements, causing the trends to vary. Here, we had difficulty achieving the perfect distribution of the components in the composite filters, which was confirmed by the contact angle with different solvents dropped onto the filter surfaces, as seen in Table 1.

Contact angles lower than 90° for water drops spread over surfaces indicate a hydrophilic nature. According to the data in Table 1, the addition of 30 % SH to BP provided BP-SH30, a filter with a contact angle higher than 90° , indicating a hydrophobic surface. The presence of proteins in SH might have contributed to the hydrophobicity of this filter. The addition of 30 % SBF to BP also made the filter surface more hydrophobic.

Using the contact angle and surface tension values of the solvents allowed us to obtain the surface free energy (γ_s) of the filters by using the Owens-Wendt-Kaelble equation (Equation 1). The results are shown in Table 1.

As mentioned by Kwok *et al.* [27], the unit areas of free energy of adhesion are thermodynamically related to the work required to separate them at the interface.

Based on the data in Table 1, the surface free energies (γ_s) ranged from 27.5 to 53.7 mJ m^{-2} , evidencing how both the amount and nature of the components affected the composite energy surfaces. The γ_s values remained between 50.0 and 60.0 mJ m^{-2} for BP, agreeing with the literature [28, 29]. The presence of CNF and BP in the filter raised the γ_s values, with BP contributing more significantly to the process. Both CNF and BP are cellulose; however, CNF has nanofiber dimensions, which can lead to better aggregation via hydrogen bonds, decreasing its contribution to the surface energy value on the surface. In this way, the surface energy tends to decrease due to decreased adhesion force on the surface. This was corroborated by comparing the γ_s values of the filters BP-CNF15 and BP—the presence of CNF decreased the surface energy.

Table 1. Mean contact angles and surface free energy data for the filters.

Filters	Mean contact angle (degrees)				Surface energy (mJ m^{-2})			
	Water	EG	DIIM	DMF	γ_s^p	γ_s^d	γ_s	R
CNF	69.1 ± 1.30	43.3 ± 1.07	40.7 ± 2.34	19.2 ± 0.890	19.9	16.0	35.9	0.971
BP	47.7 ± 0.69	35.2 ± 1.05	65.1 ± 1.15	23.1 ± 0.59	6.5	47.2	53.7	0.984
BP-CNF15	64.4 ± 3.21	59.3 ± 1.28	44.7 ± 4.44	21.5 ± 1.70	38.0	3.0	41.0	0.915
BP-SH30	94.2 ± 0.47	73.7 ± 3.45	41.3 ± 4.13	27.7 ± 0.72	19.6	7.9	27.5	0.942
BP-SBF30	78.2 ± 0.98	66.4 ± 3.14	36.0 ± 2.70	20.0 ± 1.68	15.0	13.1	28.1	0.917
CNF-BP-SH30	80.9 ± 2.41	58.7 ± 5.62	36.1 ± 5.81	21.3 ± 1.90	17.9	9.9	27.8	0.920
BP-CNF-SH30	57.1 ± 1.12	38.6 ± 1.09	52.4 ± 1.68	20.5 ± 1.61	11.3	31.9	43.2	0.977

EG = ethylene glycol, DIIM= diiodomethane, and DMF = dimethylformamide

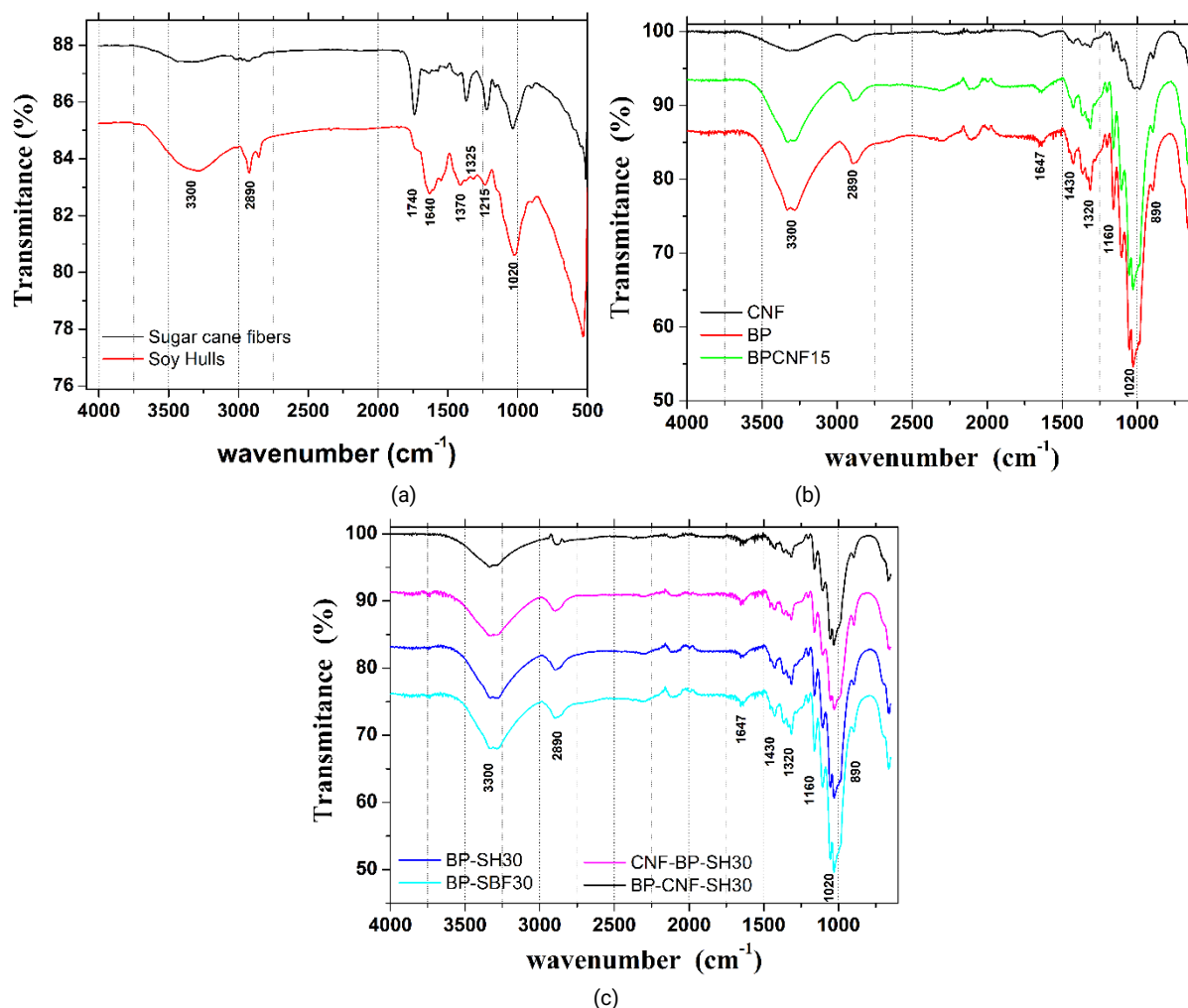


Fig. 2. FTIR-ATR of cellulosic components. (a) Sugarcane bagasse fibers and soy hulls. (b, c) lignocellulosic filters.

The addition of SH and CNF, which are “in nature” residues and with SH has a high content of lignin as well as proteins, reduced the γ_s values. Estimating the γ_s value by contact angle is very sensitive to the chemical environment of the surface itself. As mentioned by Belgacem and Gandini [30], the surface energy measured by inverse gas chromatography (IGC) can increase by almost 50 % after small molecules are removed from the surface.

The components SH, SBF, and BP used for preparing the filters had not been subjected to an appropriate process for removing surface contaminants. An ultra-homogenizing mixer was used to defibrillate the components during the filter production stage, which may have contributed to leaving small molecules anchored on the surface of the cellulosic fibers.

The surface tension of a liquid also changes in the presence of other molecules and ions. The surface tension of liquid water changed after Cd (II) and Cu (II) were added to measure the contact angle on the filter surfaces. This influence can be observed in Table 2, which lists the contact angles of the Cd (II) and Cu (II) solutions on the filter surfaces.

Depending on the nature of the components in the filter, the contact angle of Cd (II) is higher; in other cases, the contact angle of Cu (II) is higher. If the filter consists of pure cellulose, then the filter is CNF or BP. The filter CNF had a larger contact angle for Cu (II) than for Cd (II). However, for the filter BP, the contact angle values revealed that both solutions

were well spread on the fiber surfaces. An increase in the CNF content in filter BP increased the contact angle of both metal ion solutions, as expected. The presence of SBF in filter BP favored Cu (II) and Cd (II) spreading more than the presence of SH.

Table 2. Contact angles of Cd (II) and Cu (II) onto filter surfaces from 25 mg.L⁻¹ aqueous solutions.

FILTERS	CD (II)	CU (II)
CNF	77.1 ± 2.72	94.4 ± 0.17
BP	32.5 ± 1.46	22.3 ± 0.12
BP-CNF15	74.9 ± 2.67	69.5 ± 0.48
BP-SH30	94.7 ± 2.18	108 ± 1.34
BP-SBF30	34.9 ± 1.53	36.3 ± 0.93
CNF-BP-SH30	42.3 ± 0.87	100 ± 0.35
BP-CNF-SH30	41.1 ± 1.07	36.6 ± 1.66

2.4 BET

The removal process depends not only on the nature of the fibers but also on pore morphology and size. The easy flow of solutions within the filter structures increases the flow rate, permeability, and possibly contaminant removal efficiency. Therefore, BET analysis was performed and the results of relative pressure (P/P₀) versus the amount of adsorbed N₂ gas are shown in Figure 3 and Table 3.

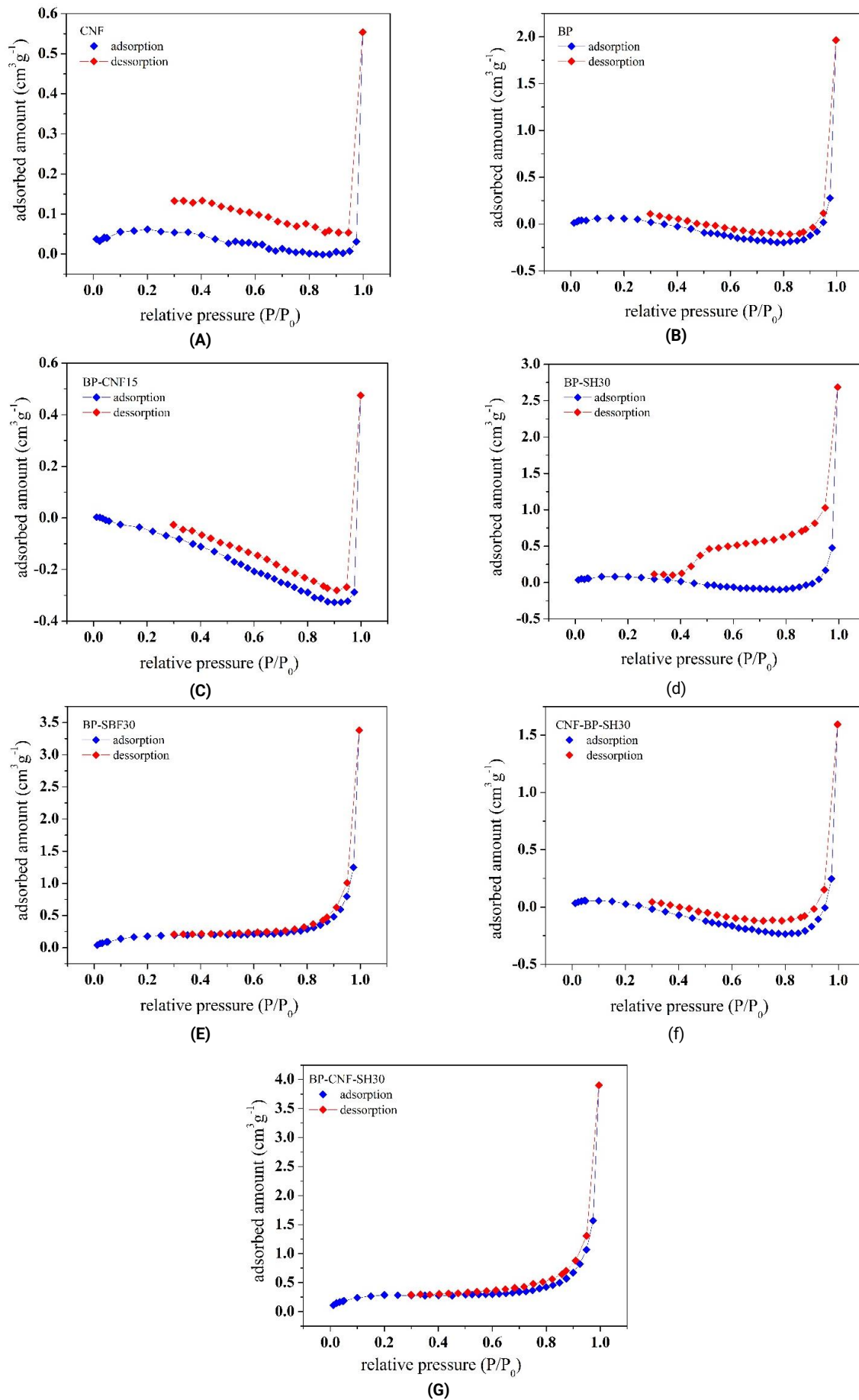


Fig. 3. N_2 adsorption-desorption curves at 77 K for the filters (a) CNF, (b) BP, (c) BP-CNF15, (d) BP-SH30, (e) BP-SBF30, (f) CNF-BP-SH30, and (g) BP-CNF-SH30.

These results allowed us to understand the morphologies of the composite filters better.

As it will be seen later, the filtration data revealed that the BET technique is not suitable for measuring the pores of these filters, but it served as a complementary technique that evidenced the contribution of nanopores to metal ion removal.

The adsorption isotherm profiles, classified according to IUPAC, are shown in Figure 3. It was found some type II and some type IV isotherms, are associated with non-porous or macroporous and mesoporous materials, respectively. According to Rouquerol *et al.* [31] the presence of a hysteresis loop is characteristic of mesoporous materials. The exception was BP-SH30, classified as macroporous. Table 3 shows the surface area and pore volume data.

Table 3. Surface area (SBET), total pore volume (Vp), and average pore diameter (dp).

Samples	S _{BET} (m ² g ⁻¹)	V _p (cm ³ g ⁻¹)	d _p (nm)
CNF	0.143	0.0006	17.3
BP	n.d.	0.0021	n.d.
BP-CNF15	n.d.	0.0003	n.d.
BP-SH30	0.116	0.0034	117
BP-SBF30	0.600	0.0041	27.2
CNF-BP-SH30	n.d.	0.0018	n.d.
BP-CNF-SH30	0.768	0.0048	25.4

n.d.: no data, possible presence of volatile components that interfered in the measurements.

The filter made of pure CNF had the smallest average pore diameter, around 17 nm. Nevertheless, the presence of BP in the filter composition increased pore size, as evidenced by the SEM images k, l in Figure 1, for CNF-BP-SH30, and m, n in Figure 1, for BP-CNF-SH30.

Filters BP, BP-CNF15, and CNF-BP-SH30 showed negative surface areas, identified in Table 3 as n.d. This suggested the

presence of volatile components, which possibly increased the volume of desorbed components during N₂ desorption, with this volume being larger than the volume of adsorbed components. Plant cells have conducting vessels and can accumulate liquids, so this type of physical structure makes losing liquids from the piths difficult. This suggests that this type of material should be submitted to an additional treatment at a higher temperature and for a longer time. The problem is that if the volatiles degrade at higher temperatures, pore contraction/expansion may occur, which would affect pore volume determinations.

For the other filters, specific surface areas ranged from 0.120 to 0.760 m² g⁻¹.

V_p indicates the porosity of the material: the greater the pore volume, the greater the porosity. Filters BP-SBF30 and BP-CNF-SH30 were the most porous among the analyzed materials. The adsorption/desorption isotherm profiles of these filters can be classified as type II isotherms.

In the work of Moubarik and Grimi [32] with sugarcane bagasse biosorbents, applied to remove Cd (II) from an aqueous solution, the maximum surface area and porosity values were 0.487 m² g⁻¹ and 57.2 nm, respectively. Similarly, Ai *et al.* [33] used sugarcane bagasse treated with nitric acid to remove Cd (II), to obtain a surface area of 0.070 m² g⁻¹; these authors did not report the porosity value. These values agree with the values reported herein for SB.

2.5 Filtration

Table 4 lists filtration data for Cu (II) solutions. The filtration times varied from 3 to 600 seconds. BP-enriched filters were the fastest. The filtration time is also considered the contact time between the adsorbate and the adsorbent, so the removal process does not depend on the contact time, but mainly on the chemical nature of the components present in the filters. This can be verified by the removal values obtained for BP-enriched, which provided the shortest filtration times and the highest Cu (II) removals.

Table 4. Filtration parameters of the filters: time (s), outflow (L h⁻¹), permeate flow (L h⁻¹ m⁻²), and Cu (II) removal (%).

Filter	Filtration time (s)	Outflow (L h ⁻¹)	Permeate flow (L h ⁻¹ m ⁻²)	Cu (II) eluted concentration (mg L ⁻¹)	Removal (%)	Removal (μmol)	Accumulated (%)
CNF	480	0.150	83	26.5	4.6	0.399	19.0
	600	0.120	67	25.6	7.8	0.684	
	600	0.120	67	25.9	6.6	0.580	
BP	4	18.0	10,000	20.5	26.2	2.29	36.7
	4	18.0	10,000	25.7	7.3	0.640	
	4	18.0	10,000	26.8	3.2	0.282	
BP-CNF15	7	10.3	5,714	22.3	19.7	1.72	28.3
	8	9.00	5,000	26.1	5.9	0.512	
	8	9.00	5,000	27.0	2.7	0.236	
BP-SH30	3	24.0	13,333	24.2	12.6	1.10	31.3
	3	24.0	13,333	25.4	8.5	0.738	
	3	24.0	13,333	24.9	10.2	0.891	
BP-SBF30	3	24.0	13,333	23.2	16.2	1.42	30.5
	3	24.0	13,333	25.6	7.8	0.678	
	3	24.0	13,333	25.9	6.5	0.568	
CNF-BP-SH30	60	1.20	667	24.8	10.4	0.908	30.1
	160	0.450	250	24.8	10.7	0.937	
	200	0.360	200	25.2	9.0	0.787	
BP-CNF-SH30	6	12.0	6,667	23.2	16.4	1.43	46.5
	7	10.3	5,714	23.4	15.5	1.36	
	7	10.3	5,714	23.7	14.6	1.28	

The low pressure involved in the filtration evidenced that the filters containing higher levels of CNF provided the lowest values of permeate flow – considering the three filtration steps, they were 83, 67, and 67 L h⁻¹ m⁻², respectively. It was observed a 160-fold increase in the filtration capacity for filters BP-SH30 and BP-SBF30 compared to CNF. Both BP-SH30 and BP-SBF30 had a permeate flow of 13,333 L h⁻¹ m⁻². Additionally, the BP-enriched filters removed almost four times more Cu (II) than CNF when the first filtration step was considered.

After three consecutive filtration steps, Cu (II) removal decreased probably because the adsorption sites inside the filter structures were occupied or the chemical environment of the adsorbent surface changed after the cations were adsorbed. Nevertheless, CNF and BP-SH30 filters provided different results: Cd (II) removal after the first, second, and third filtration steps was 4.6, 7.8, 6.6 %, and 12.6, 8.5, and 10.2 %, respectively.

Considering the accumulated data for the three filtration steps, BP is important for enhancing Cu (II) removal from an aqueous medium. The two highest accumulated removal

values were 36.7 % and 46.5 % for filters BP and BP-CNF-SH30, respectively, with cumulative filtration times of 12 and 20 seconds.

It also studied Cd (II) removal by the filters (Table 5).

Practically, there were no differences in filtration time compared to Cu (II). Again, the filtration time increased along the sequential filtration for filters CNF and CNF-BP-SH30. Performing the third filtration step was not possible because it exceeded the time limit of 1200 seconds. For five of the seven filters, Cd (II) removal was higher than Cu (II) removal. For Cd (II) removal, the filtration time was not considered a relevant variable because it resembled what we had observed for Cu (II) removal, i.e. shorter filtration times provided higher removal rates. This implied that the nature of the components used in the filters determined the process, as observed for filters CNF-BP-SH30 and BP-CNF-SH30, which removed 58.2 % and 77.2 % Cd (II), respectively.

The permeate flow rate decreased when the amount of CNF in the filter increased. Filters CNF and CNF-BP-SH30 had a maximum permeate flow of 222 L.h⁻¹.m⁻², while the best filters provided 60-fold higher values, 13,333 L h⁻¹ m⁻².

Table 5. Filtration parameters of the filters: time (s), outflow (L h⁻¹), permeate flow (L h⁻¹ m⁻²), and Cd (II) removal (%).

Filter	Filtration time (s)	outflow(L h ⁻¹)	Permeate flow (L h ⁻¹ m ⁻²)	Cd (II) eluted concentration (mg L ⁻¹)	Removal (%)	Removal (μmol)	Accumulated (%)
CNF	180	0.40	222	31.5040	5.3	0.314	12.4
	900	0.08	44	30.9133	7.1	0.419	
BP	----(*)	----	----	----	----	----	25.6
	3	24.0	13,333	28.0	15.8	0.933	
	3	24.0	13,333	31.3	5.9	0.351	
	3	24.0	13,333	32.0	3.9	0.232	
BP-CNF	8	9.00	5,000	26.0	21.9	1.30	33.7
	8	9.00	5,000	30.6	8.0	0.471	
	8	9.00	5,000	32.0	3.8	0.227	
BP-SH30	3	24.0	13,333	28.8	13.5	0.800	39.1
	3	24.0	13,333	28.6	14.1	0.834	
	3	24.0	13,333	29.5	11.5	0.678	
BP-SBF30	3	24.0	13,333	28.6	13.9	0.823	36.4
	3	24.0	13,333	29.4	11.5	0.680	
	3	24.0	13,333	29.6	11.0	0.645	
CNF-BP-SH30	180	0.400	222	27.8	16.4	0.971	58.2
	900	0.080	44	26.0	21.9	1.30	
	1200	0.060	33	26.7	19.9	1.18	
BP-CNF-SH30	7	10.3	5,714	24.4	26.7	1.58	77.2
	7	10.3	5,714	24.1	27.4	1.62	
	7	10.3	5,714	25.6	23.1	1.37	

(*) Filtration time exceeded.

The bivalent metallic cations interacted with identical surfaces of cellulosic filters during the filtration steps. Cu (II) has an ionic radius of 0.73 Å, whereas Cd (II) has an ionic radius of 0.97 Å, that is, 1.3-fold larger than the Cu (II) ionic radius. As mentioned by Salam *et al.* [34] cations that have smaller ionic radii penetrate networks and interstices more easily and adsorb on surfaces. This was confirmed by five samples. The only exceptions were CNF-BP-SH30 and BP-CNF-SH30, which removed more Cd (II) than Cu (II).

Considering the accumulated value in micromol (μmol) for Cu (II), the removal sequence for the three best filters were BP-CNF-SH30 > CNF-BP-SH30 > BP-SH30 with 4.6, 3.4, and 2.3 μmol of Cu (II) removal, respectively.

Vitas *et al.* [35] used chemically modified beech wood to produce biosorbent materials for removing Cu (II). The removal through adsorption was performed in the batch mode for 24 h, and the highest removal was 2.82 ± 0.04 mmol of COOH/g of wood. Here, about 51 % Cu (II) was removed within 7 seconds of filtration, demonstrating the fast and great removal potential that our lignocellulosic composite filters represent.

Lee and Rowell [36] tested several lignocellulosic raw materials like spruce, coconut core, sugarcane bagasse, kenaf bast, kenaf core, and cotton to remove toxic metals like Cu (II), Ni (II), and Zn (II) from aqueous solutions. They observed that the amount of removed metal and the lignin content were not related. Moreover, Reddad *et al.* [37] discussed the important

effect of hemicelluloses on metal ion sorption due to the presence of ionizable carboxylic acid groups in the uronic acids.

Çifci and Sanli [38] studied Cu (II) and Cd (II) removal by the crossflow filtration technique through Alginate Acid/Cellulose Composite Membranes with a filtration area 1.7-fold larger than the filtration area of the cellulosic filters used herein. The authors found a permeate flow smaller than $2,000 \text{ L h}^{-1} \text{ m}^{-2}$. They obtained retention percentages of about 60 % in 900 seconds (15 min) from contaminant solutions containing 6.36 and 11.2 mg L^{-1} Cu (II) and Cd (II), respectively. Therefore, our filters presented excellent removal capacity under low-pressure conditions.

In another work, a cellulose filter paper was chemically modified by esterification with EDTA dianhydride. For analysis, the authors used solutions with 2 mg in 20 mL of Cd (II) and Cu (II). Cd (II) removal was 96 % after 3,600 s (60 min); Cu (II) removal was 90 % after 5,400 s (90 min). Although there was no filtration during the removal, the results showed how cellulosic components are efficient at metal removal [39].

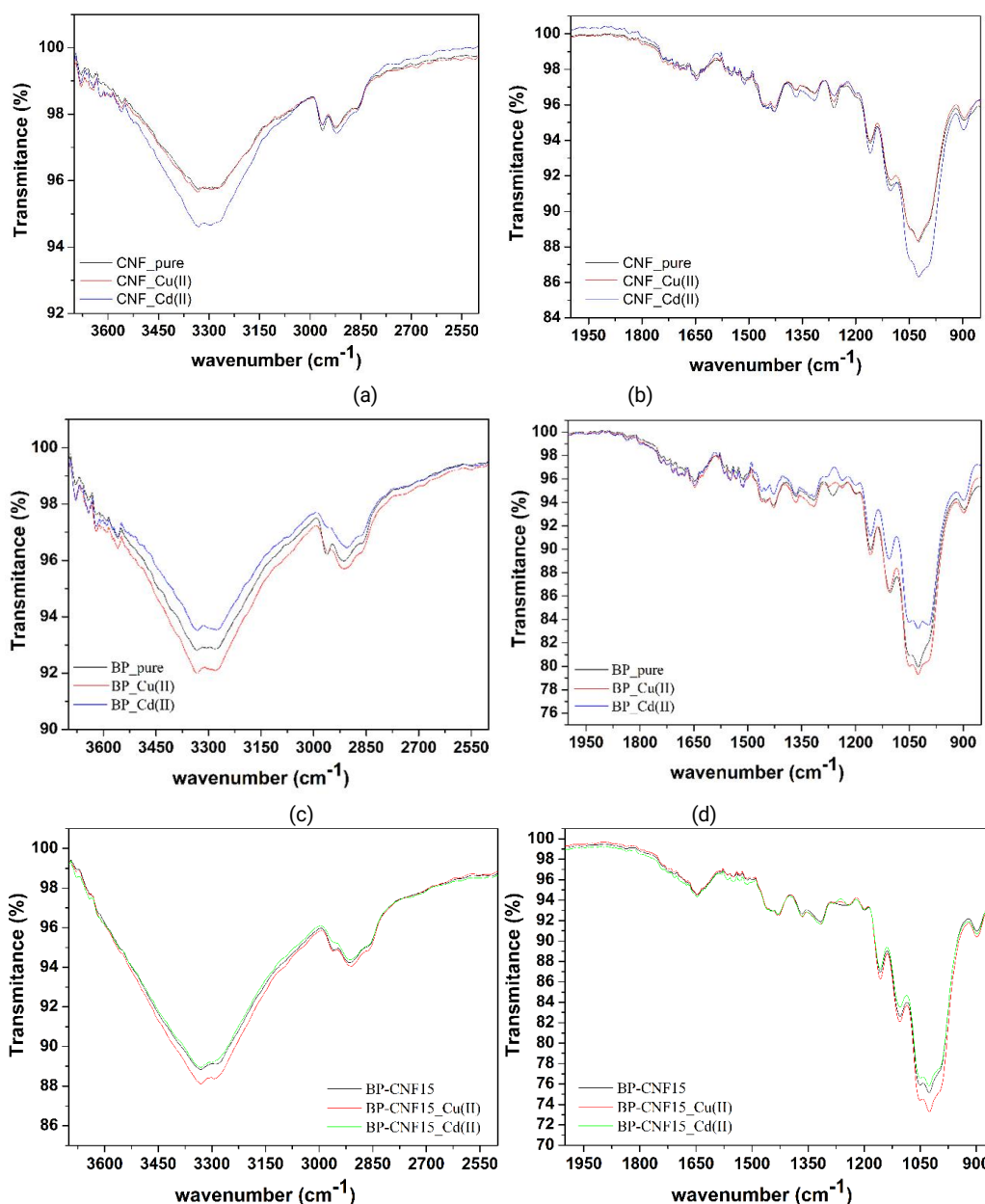
Jiang et al. [40] studied Cu (II) removal with bagasse

modified with acrylonitrile and hydroxylamine. Depending on the Cu (II) concentration, 6,000 s (100 min) and a concentration of $1.52 \text{ mg } 20 \text{ mL}^{-1}$ solution provided the removal of approximately 22 mg g^{-1} adsorbent.

The use of hulls as a raw material for removing contaminants has also shown good potential. A pretreated rice hull was used as biosorbent for Cu (II) and Cd (II) removal. The maximum amount of removal was 8.89 and 1.58 mg g^{-1} for Cu (II) and Cd (II), respectively, after 1,800 s (30 min) [41].

2.6 Metallic cationic interactions

The interaction of metallic cations, Cd (II) and Cu (II), with the lignocellulosic filters using FTIR in ATR mode (see Figure 4), allowed us to verify that there were changes in the positions of the signals, alteration of the signal shape, increasing or decreasing in the intensity of the bands and the broadening of the signal. These changes refer to the respective signals before and after contact with metallic cations.



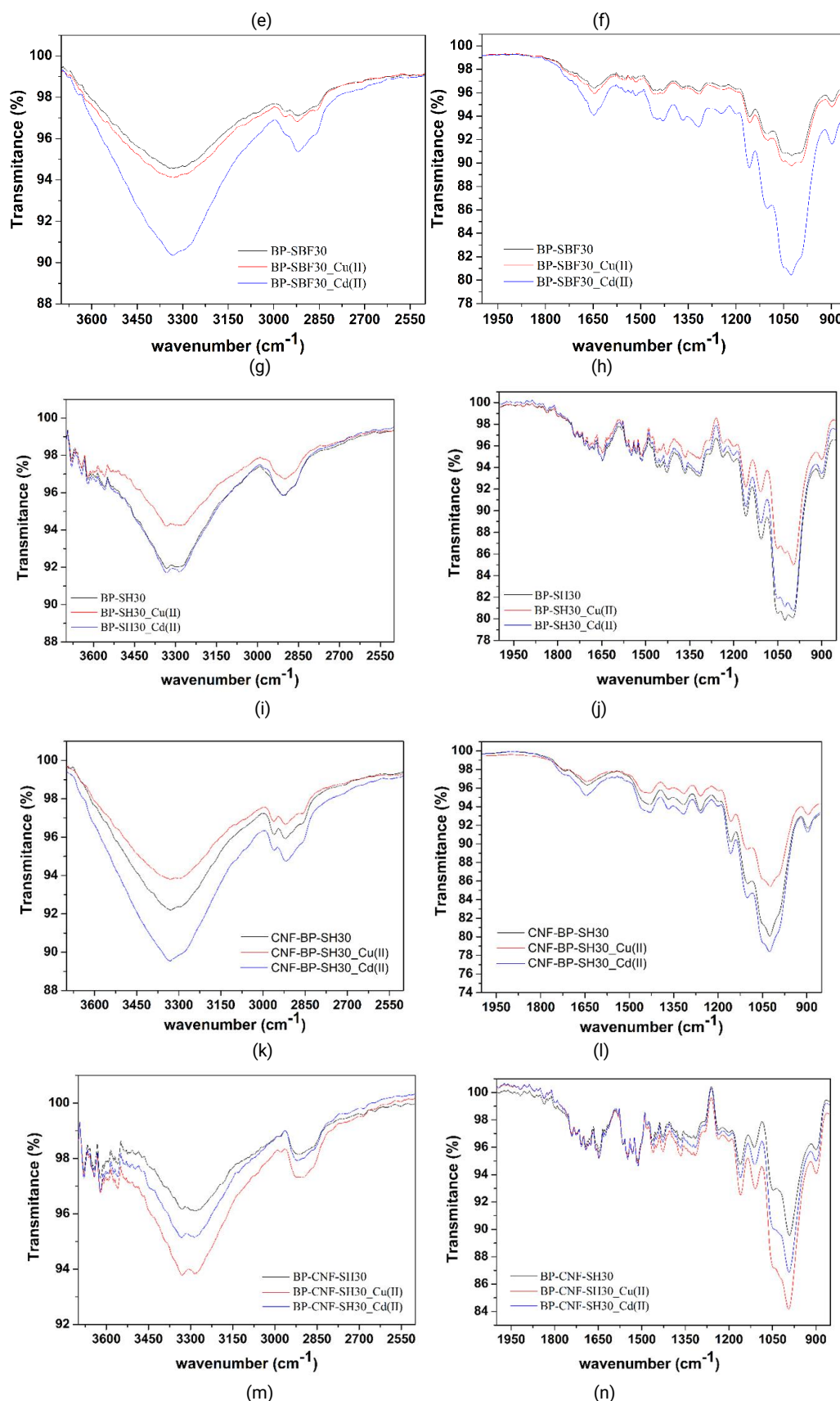


Fig. 4. Metallic cations interaction with lignocellulosic filters by FTIR-ATR. Spectra (a, c, e, g, i, k, m) range from 3700 to 2500 cm^{-1} , and 4(b, d, f, h, j, l, n) range from 2000 to 850 cm^{-1} .

The most chemical groups affected by Cu (II) and Cd (II) interactions were mainly found in the regions of 3300, 1647, 1370, 1316, 1280, 1260, 1240, 1200, 1160, 1025, and 990 cm^{-1} .

Interactions between metal cations and cellulosic adsorbents can occur, most commonly, through ionic interactions, coordination by complexation, and intermolecular forces. These interactions can be noticeable

through the FTIR spectrum, however, in some cases, the interactions are very discreet or difficult to perceive [42].

In this study, the interactions between Cd (II) and Cu (II) with cellulosic components were very evident, as seen in Figure 4.

Figure 5 shows the most probable groups that interact with Cd (II) and Cu (II) using observations from FTIR.

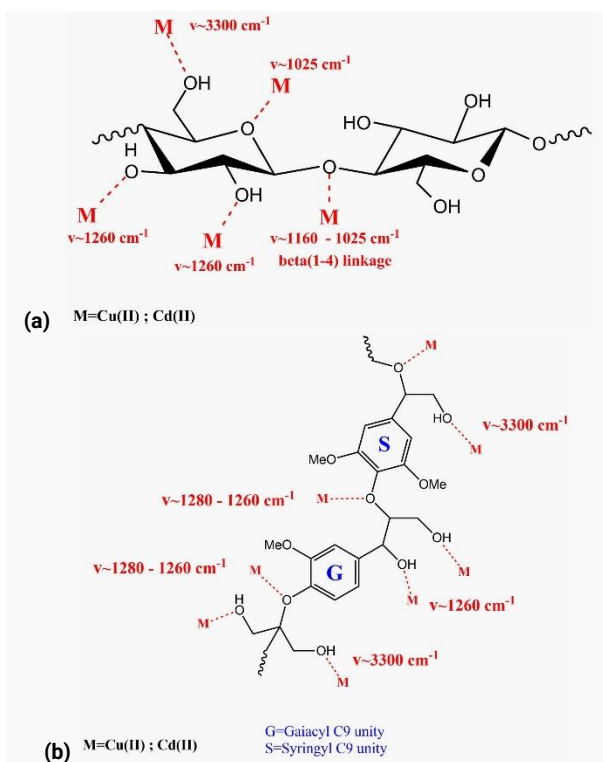


Fig. 5. Most likely interactions between metallic cations and chemical groups are based on FTIR information. (a) components enriched in cellulose. (b) components containing cellulose, lignin, and hemicellulose.

The filters used in this work are made of enriched cellulose and cellulose, lignin, and hemicellulose. The latter are filters made with sugarcane bagasse fibers and soybean hulls, both "in nature".

Figure 5-a shows that in components enriched with cellulose, not only do interactions with metal cations occur via hydroxyl groups, but they also occur with oxygen as a heteroatom in the anhydroglucose ring. As well, it occurs with the oxygen between the glycosidic rings, more specifically as part of the β (1-4) bond.

Figure 5-b allows us to understand how the interactions between Cd (II) and Cu (II) occur using a model of fragments of syringyl and guaiacyl units, present in lignin from soybean hulls and sugarcane bagasse fibers. Despite being a more rigid structure than cellulose, the three-dimensional structure of lignin contains a variety of in-plane and out-of-plane groups about the C9 units, this allows several interactions to occur with these cations. The changes in signal intensities and band broadenings reflect the vibrational changes undergone in the presence of these metallic cations.

In other works, similar results were found by using FTIR to study interactions between chemical groups and metallic cations [16, 43].

3. Material and Methods

3.1. Preparation of agro-industrial residues

The company Suzano (São Paulo, Brazil) provided the eucalyptus cellulose nanofibers (CNF, as 3 % (w/w) aqueous dispersion) and the bleached pulp (BP). Usina Vale do Tijuco (Uberaba, Brazil) provided the sugarcane bagasse fibers (SBF). Algar Agro S.A. (Uberlândia, Brazil) supplied the soy hulls (SH).

SH and SBF were washed to eliminate residual dirt. Then, they were crushed in an industrial blender for 2 min. Next, the dried crushed samples were separated by granulometry; sieves with openings between 12 and 35 mesh were used on a shaking table for 15 min, at maximum power. Finally, the fraction retained in the 35-mesh sieve was separated and used for preparing the filters.

The SH and SBF were washed with 500 mL of distilled water at 70 °C and filtered. This process was repeated two more times. After drying, the samples were submitted to Soxhlet extraction with cyclohexane for 8 h. The samples were placed in an oven at 60 °C for 4 h and 105 °C for 2 h and stored in desiccators.

3.2. Preparation of filters

Filters weighing 1.20 g were prepared from the following components: CNF, BP, SH, and SBF. To prepare filters consisting of pure CNF or pure PB, wet masses of 40.0 g (3 % in solid), representing 1.20 g, were weighed. The SH or SBF proportion in the composite filters was kept constant. To keep the filters with the same total mass, the following procedure was used. The sum of the masses of all the components was 1.20 g. When SH or SBF was added, they represented 30 % (0.360 g) of the total mass; the remaining 70 % (0.840 g) was completed with a mixture of CNF and BP. To exemplify the amounts of these components in the mixture, filter BP-CNF-SH30 had 0.360 g of SH, 0.714 g of CNF, and 0.126 g of BP. For the filter made of pure CNF or PB, the samples were added to a beaker containing 360 mL of distilled water under stirring for 10 min. Then, the dispersion was placed in a Buchner filter with a polyester mesh at the bottom, and the apparatus was connected to a Kitasato flask, which in turn was connected to a vacuum pump. After the liquid was drained, the solid mass on the filter fabric was removed with the aid of tweezers and dried in an oven at 60 °C for 4 h and at 105 °C for 4 h. This procedure was also followed for mixtures of BP/CNF and BP/CNF containing SH or SBF.

Symbols of the Filters: BP (1.20 g), CNF (1.20 g), BP-CNF15 {(85 % BP (1.02 g) + 15 % CNF (0.180 g)), BP-SH30 {(70 % BP (0.840 g) + 30 % SH (0.360 g)), BP-SBF30 {(70 % BP (0.840 g) + 30 % SBF (0.360 g)), CNF-BP-SH30 {(85 % (0.714 g) CNF + 15 % BP (0.126 g) + 30 % SH (0.360 g)), and BP-CNF-SH30 {(85 % BP (0.714 g) + 15 % CNF (0.126 g) + 30 % SH (0.360 g))}.

3.3 Contaminant removal

A Manifold-type apparatus consisting of a 300-mL container flask (to which the contaminated solution was added), a porous base (over which the filter was placed), and a collector flask (with an inlet for connecting a vacuum pump connected to a pressure gauge) was employed. The filters were cut into 48-mm diameter pieces and tested. In each test, one piece of the filter was placed between the container flask and the porous base. A volume of 60 mL of the Cd (II) solution (or Cu (II)) was divided into three fractions of 20 mL of Cd (II). The first fraction was added to the container, the vacuum pump was immediately turned on, and the filtration time was recorded. The filtered fraction was kept for further analysis.

The procedure was then repeated twice for the same filter so that three cycles of filtration were conducted for each filter. The obtained parameters were used for determining the filtration time (s), outflow (L h⁻¹), permeate flow (L h⁻¹ m⁻²), eluted concentration (mg L⁻¹), and removal (%).

The Cd (II) stock solution was 33.3 mg L⁻¹, which implied that there were 5.92 μmol of Cd (II) in 20 mL. Similarly, the Cu (II) stock solution was 27.7 mg L⁻¹, which implied that there were 8.73 μmol of Cu (II) in 20 mL. Filtration times that exceeded 20 min (1200 s) were disregarded for analysis.

3.4. Characterization of filters

3.4.1 SEM with EDS

Cross-sectional images of the filters were analyzed by using a scanning electronic microscope (SEM) ZEISS model EVO MA10, at magnitudes of 500 and 3 KX; the working distance was fixed at 11.5 mm. The samples were cold-fractured with liquid nitrogen.

3.4.2 Infrared spectroscopy (FTIR)

The filters were analyzed by FTIR in the ATR mode on a Perkin Elmer Spectrophotometer Two model. The spectra were recorded from 4000 to 400 cm⁻¹, with 20 scans.

In another experiment, the filters were placed in contact with 11 ppm solutions of Cd (II) and Cu (II), then washed to remove excess metal ions and placed to dry in an oven at 60 °C for 6 hours and at 110 °C for 2 hours. After this step, FTIR analyses were carried out in an IRPrestige-21 device (Shimadzu) with the PIKE MIRacle Total Attenuated Reflectance (ATR) accessory. The samples were measured in the region between 4000 and 600 cm⁻¹, with 20 scans and a resolution of 2.0 cm⁻¹. The results allowed us to better understand the interactions between these metallic cations and the filter components.

3.4.3 Contact angle

The contact angle was measured on a Theta Lite Optical Tensiometer TL100 with a CCD of 60 frames per second. Drops with an approximate volume of 5 μL of ultra-pure water (γ_L = 72.80 mN/m; γ_{LP} = 51.00 mN/m), diiodomethane (γ_L = 49.5 mN/m; γ_{LP} = 1.30 mN/m), and ethylene glycol (γ_L = 48.00 mN/m; γ_{LP} = 19.00 mN/m) were measured, in triplicate. Based on the data of the mean angles obtained by the analysis and dispersive and polar energies of the liquids, it was possible to calculate the dispersive (γ_{PL}) and polar (γ_{DL}) surface energies of the composite filters by using Equation 1 of the Owens-Wendt-Kaelble equation [27].

$$\frac{\gamma_L(1+\cos\theta)}{2\sqrt{\gamma_L^D}} = \sqrt{\gamma_S^D} + \sqrt{\gamma_S^P} \sqrt{\frac{\gamma_L^P}{\gamma_L^D}} \quad (\text{Eq.1})$$

where: θ = angle of the liquid drop on the solid surface (degrees); γ_L = total energy of the liquid (mJ m⁻²); γ_{LD} = dispersive energy of the liquid (mJ m⁻²); γ_{LP} = polar energy of the liquid (mJ m⁻²); γ_{SD} = dispersive energy of the solid (mJ m⁻²); and γ_{SP} = polar energy of the solid (mJ m⁻²).

3.4.4 BET analysis

The surface area and porosity of the samples were evaluated by N₂ adsorption isotherms at -195.5 °C in an automatic physisorption instrument ASAP2020 plus (Micromeritics, Norcross, GA, USA) over a relative pressure

(P/P₀) range from about 0 to 0.995. Before the measurements, all the samples were degassed at 90 °C for 12 h under vacuum. The specific surface area (SBET) was determined by the Brunauer-Emmett-Teller (BET) method; adsorption data in the P/P₀ range from 0.05 to 0.30 were used. The main pore diameter (dp) was calculated by the BJH method (dP = 4Vp/SBET, where Vp is the total pore volume). The total pore volume was calculated by converting the amount of N₂ adsorbed at a P/P₀ of 0.995 to the volume of liquid adsorbate [44].

4. Conclusions

Filters made of lignocellulosic residues are promising biosorbents. The surface free energy of the filter increases with an increasing amount of Bleached Pulp (53.7 mJ m⁻²). However, the addition of bagasse fibers (28.1 mJ m⁻²) and soy hull (27.5 mJ m⁻²) decreases the surface free energy.

The contact time is not the main variable that helps to explain the Cu (II) and Cd (II) removal processes. The ionic radii of the cations are important for five filters. The exceptions are BP-CNF-SH30 and CNF-BP-SH30.

Filters BP-SH30 and BP-SBF30 have identical permeate flow, 13,333 L h⁻¹ m⁻², and can remove 39.1 % and 36.4 % Cd (II), and 31.3 %, and 30.5 % Cu (II), respectively.

A study of interactions using FTIR made it possible to highlight the main vibration modes that changed interactions with the Cd (II) and Cu (II) cations. In this way, it was highlighted which chemical groups most contributed to interacting with these cations involved in the filtration removal process.

The investigated filtration effects demonstrated the easy applicability of the prepared biofilters, which provide fast Cd (II) and Cu (II) removal. Hence, the use of lignocellulosic residues as raw material to produce biofilters has great potential for providing a sustainable destination, thus adding value to the agro-industrial production cycle.

Acknowledgments

The authors thank the Scanning Electron Microscopy Laboratory of the School of Chemical Engineering of the Federal University of Uberlândia (FEQUI-UFU) for the SEM analysis. The authors thank by support of this work the Minas Gerais State Foundation for Research Support -FAPEMIG, process CEX - APQ-01651-17, Brazil. The authors also thank Dr. Cynthia Maria de Campos Prado Manso, who revised and edited this text.

Author Contributions

Pedro Eduardo Costa – Investigation, Methodology. Altamiro Xavier de Souza – Data Curation, Formal Analysis. Gabriel Badagnani de Carvalho – Software, Visualization, Project Administration. Marcelo Firmino de Oliveira – Funding acquisition; Resources. Cláudio Roberto Neri – Formal Analysis; Methodology; Software. Anizio Marcio de Faria – Writing – Original Draft, Writing – Review & Editing. Daniel Pasquini - Funding acquisition; Resources. Luís Carlos de Morais – Conceptualization; Funding acquisition; Investigation; Methodology; Project administration; Resources; Supervision; Visualization; Writing – review & editing.

References and Notes

- [1] Khulbe, K. C.; Matsuura, T. *Appl. Water Sci.* **2018**, *8*, [Crossref]
- [2] WHO. Guidelines for drinking-water quality. 4th ed. Switzerland. 2011.
- [3] Ritchie, S. M. C.; Bachas, L. G.; Olin, T.; Sikdar, S. K.; Bhattacharyya, D. *Langmuir*, **1999**, *15*, 6346. [Crossref]
- [4] Malik, D. S.; Jain, C. K.; Yadav, A. K. *Appl. Water Sci.* **2017**, *7*, 2113. [Crossref]
- [5] Karim, Z.; Mathew, A. P.; Kokol, V.; Wei, J.; Grahn, M. *RSC Adv.* **2016**, *6*, 20644. [Crossref]
- [6] Sjahro, N.; Yunus, R.; Abdullah, L. C.; Rashid, S. A.; Asis, A. J.; Akhlisah, Z. N. *Cellulose* **2021**, *28*, 7521. [Crossref]
- [7] Oyewo, O. A.; Elemike, E. E.; Onwudiwe, D. C.; Onyango, M. S. *Int. J. Biol. Macromol.* **2020**, *164*, 2477. [Crossref]
- [8] Tshikovhi, A.; Mishra, S. B.; Mishra, A. K. *Int. J. Biol. Macromol.* **2020**, *152*, 616. [Crossref]
- [9] Yu, J.; Wang, A. C.; Zhang, M.; Lin, Z. *Materials Today* **2021**, *50*, 329. [Crossref]
- [10] Vasić, V.; Kukić, D.; Šćiban, M.; Đurišić-Mladenović, N.; Velić, N.; Pajin, B.; Crespo, J.; Farre, M.; Šereš, Z. *Water* **2023**, *15*, 1853. [Crossref]
- [11] Zhang, C.; Zhang, R. Z.; Ma, Y. Q.; Guan, W. B.; Wu, X. L.; Liu, X.; Li, H.; Du, Y. L.; Pan, C. P. *ACS Sustain. Chem. Eng.* **2015**, *3*, 396. [Crossref]
- [12] Ikhuria, E. U.; Okieimen, F. E. *Int. J. Environ. Stud.* **2000**, *57*, 401. [Crossref]
- [13] Okieimen, F. E.; Orhororo, F. I. *Int. J. Environ. Anal. Chem.* **1986**, *24*, 319. [Crossref]
- [14] Rana, A. K.; Mishra, Y. K.; Gupta, V. K.; Thakur, V. K. *Sci. Total Environ.* **2021**, *797*. [Crossref]
- [15] Barsbay, M.; Kavakli, P. A.; Tilki, S.; Kavakli, C.; Güven, O. *Radiat. Phys. and Chem.* **2018**, *142*, 70. [Crossref]
- [16] Fujisawa, S.; Okita, Y.; Fukuzumi, H.; Saito, T.; Isogai, A. *Carbohydr. Polym.* **2011**, *84*, 579. [Crossref]
- [17] Isogai, A.; Saito, T.; Fukuzumi, H. *Nanoscale* **2011**, *3*, 71. [Crossref]
- [18] Okita, Y.; Saito, T.; Isogai, A. *Biomacromolecules* **2010**, *11*, 1696. [Crossref]
- [19] Silva, T. A. L.; Zamora, H. D. Z.; Varão, L. H. R.; Prado, N. S.; Baffi, M. A.; Pasquini, D. *Waste Biomass Valorization* **2018**, *9*, 2191. [Crossref]
- [20] Neto, W. P. F.; Silvério, H. A.; Dantas, N. O.; Pasquini, D. *Ind. Crops Prod.* **2013**, *42*, 480. [Crossref]
- [21] Putz, K. W.; Compton, O. C.; Palmeri, M. J.; Nguyen, S. B. T.; Brinson, L. C. *Adv. Funct. Mater.* **2010**, *20*, 3322. [Crossref]
- [22] Pavithra, R.; Gunasekaran, S. *Int. J. Curr. Res. Acad. Rev.* **2015**, *3*, 42.
- [23] Moghaddam, L.; Rencoret, J.; Maliger, V. R.; Rackemann, D. W.; Harrison, M. D.; Gutiérrez, A.; Del Río, J. C.; Doherty, W. O. S. *ACS Sustain. Chem. Eng.* **2017**, *5*, 4846. [Crossref]
- [24] Łojewska, J.; Miśkowiec, P.; Łojewski, T.; Proniewicz, L. M. *Polym. Degrad. Stab.* **2005**, *88*, 512. [Crossref]
- [25] Adel, A. M.; Abd El-Wahab, Z. H.; Ibrahim, A. A.; Al-Shemy, M. T. *Carbohydr. Polym.* **2011**, *83*, 676. [Crossref]
- [26] Oh, S. Y.; Dong, I. Y.; Shin, Y.; Hwan, C. K.; Hak, Y. K.; Yong, S. C.; Won, H. P.; Ji, H. Y. *Carbohydr. Res.* **2005**, *340*, 2376. [Crossref]
- [27] Kwok, D. Y.; Neumann, A. W. *Adv. Colloid Interface Sci.* **1999**, *81*, 167. [Crossref]
- [28] Luner, P. E.; Oh, E. *Colloids Surf. A.* **2001**, *181*, 31. [Crossref]
- [29] Gardner, D. J.; Oporto, G. S.; Mills, R.; Samir, M. A. S. A. *J. Adhes. Sci. Technol.* **2008**, *22*, 545. [Crossref]
- [30] Belgacem, M. N.; Gandini, A. *Compos. Interfaces* **2005**, *12*, 41. [Crossref]
- [31] Rouquerol, J.; Llewellyn, P.; Rouquerol, F. *Stud. Surf. Sci. Catal.* **2007**, *160*, 49. [Crossref]
- [32] Moubarik, A.; Grimi, N. *Food Res. Int.* **2015**, *73*, 169. [Crossref]
- [33] Ai, S.; Huang, Y.; Xie, T.; Huang, C. *Ind. Eng. Chem. Res.* **2020**, *59*, 8795. [Crossref]
- [34] Salam, M. A.; Al-Zhrani, G.; Kosa, S. A. C. R. *Chim.* **2012**, *15*, 398. [Crossref]
- [35] Vitas, S.; Keplinger, T.; Reichholf, N.; Figi, R.; Cabane, E. *J. Hazard. Mater.* **2018**, *355*, 119. [Crossref]
- [36] Lee, B. G.; Rowell, R. M. *J. Nat. Fibers* **2004**, *1*, 97. [Crossref]
- [37] Reddad, Z.; Ge Ârente, C.; Ás, Y. A.; Ralet, M.-C.; Thibault, J.-F. È.; Le Cloirec, P. *Carbohydr. Polym.* **2002**, *49*, 23. [Crossref]
- [38] Çifci, C.; Şanlı, O. J. *Appl. Polym. Sci.* **2010**, *115*, 616. [Crossref]
- [39] D'Halluin, M.; Rull-Barrull, J.; Bretel, G.; Labrugère, C.; Le Grogneq, E.; Felpin, F. X. *ACS Sustain. Chem. Eng.* **2017**, *5*, 1965. [Crossref]
- [40] Jiang, Y.; Pang, H.; Liao, B. *J. Hazard Mater.* **2009**, *164*, 1. [Crossref]
- [41] Li, W. C.; Law, F. Y.; Chan, Y. H. M. *Environ. Sci. Pollut. Res.* **2015**, *24*, 8903. [Crossref]
- [42] Li, M.; Ashagre Messele, S.; Boluk, Y.; El-Din, M. G. *Carbohydr. Polym.* **2019**, *221*, 231. [Crossref]
- [43] Mizuguchi, M.; Nara, M.; Kawano, K.; Nitta, K. *FEBS Lett.* **1997**, *417*, 153. [Crossref]
- [44] Brunauer, S.; Emmett, P. H.; Teller, E. *J. Am. Chem. Soc.* **1938**, *60*, 309. [Crossref]

How to cite this article

Costa, P. E.; de Souza, A. X.; de Carvalho, G. B.; Pasquini, D.; de Oliveira, M. F.; de Faria, A. M.; Neri, C. R.; de Moraes, L. C. *Orbital: Electron. J. Chem.* **2024**, *16*, 98. DOI: <http://dx.doi.org/10.17807/orbital.v16i2.19863>